

Supporting Information to “The nature of sodium atoms/(Na⁺,e⁻) contact pairs in liquid tetrahydrofuran”

William J. Glover, Ross E. Larsen, and Benjamin J. Schwartz*

Department of Chemistry and Biochemistry, University of California, Los Angeles, Los Angeles, CA 90095-1569

CONSTRAINING TETRAHYDROFURAN TO BE RIGID AND PLANAR

In our simulation model, tetrahydrofuran (THF) is constrained to be a rigid and planar molecule. Our previous simulations of THF solutions[1–4] used a modified SHAKE algorithm[5] to handle these constraints; however, our previous simulations were based on the Verlet integrator, so that our previous approach was not readily extendible to the present simulations, which require the velocity Verlet integrator.[6] We thus followed the ideas of Feenstra, Hess and Berendsen[7] and enforced the rigid planarity of THF via three dummy atoms, which when constrained to form a rigid triangle, completely determine the molecular geometry of THF. In other words, the dummy-atom positions form a basis in which the location of any regular THF atom becomes:

$$\vec{r}_i = (1 - a_i - b_i)\vec{r}_{d1} + a_i\vec{r}_{d2} + b_i\vec{r}_{d3}, \quad (1)$$

where \vec{r}_i is the position of THF atomic site i (of which there is one oxygen site, two α -methylene and two β -methylene sites); \vec{r}_{d1} , \vec{r}_{d2} and \vec{r}_{d3} are the positions of the dummy atoms; and a_i and b_i are expansion coefficients. For the particular choice of dummy atoms positions described below, the expansion coefficients are given in Table I.

With the THF atomic site positions fully determined, the dummy atoms become the only THF degrees of freedom that are propagated in the constrained molecular dynamics simulation, with the forces on these atoms redistributed from the original atoms:

$$\begin{aligned} \vec{F}_{d1} &= \sum_i (1 - a_i - b_i) \vec{F}_i \\ \vec{F}_{d2} &= \sum_i a_i \vec{F}_i \\ \vec{F}_{d3} &= \sum_i b_i \vec{F}_i, \end{aligned} \quad (2)$$

where \vec{F}_{dj} is the force on dummy atom j (taking on values 1 to 3) and \vec{F}_i is the force on THF atom i . The distances between the dummy atoms are constrained with the RATTLE algorithm.[8] In order that the dynamics of THF be unaltered, the masses and positions of the dummy atoms were chosen such that the total mass, center of mass and moment of inertia tensor of THF remained the same as the original molecular model. This leaves one remaining degree of freedom, so we selected the first dummy atom to correspond to the position of the THF oxygen site. The position and masses of the THF dummy atoms are presented in Table II. In summary, the dummy-atom construction replaces our previous use[1–4] of the Ciccotti approach[5] for maintaining the rigid planarity of the THF molecules, allowing us to use the velocity-Verlet integrator.

TABLE I. Expansion coefficients for THF atomic sites

Site i	a_i	b_i
O	0.0	0.0
$C_{\alpha 1}$	0.74387310	-0.32139386
$C_{\alpha 2}$	-0.32139386	0.74387310
$C_{\beta 1}$	0.95161158	0.25123302
$C_{\beta 2}$	0.25123302	0.95161158

TABLE II. Positions and masses of THF dummy atoms

Site j	\vec{r}_{dj} (Å) ^a	M_j (u) ^b
d1	(0.0, 1.1962017)	26.510565
d2	(1.0915968, -0.69548652)	22.798417
d3	(-1.0915968, -0.69548652)	22.798417

^a Position of dummy site j (in plane of molecule).

^b Mass of dummy site j in atomic mass units.

MOLECULAR DYNAMICS SNAPSHOTS FOR TCP COORDINATION NUMBERS

In the main text, we presented molecular dynamics snapshots of the four-coordinate sodium tight-contact pair (TCP) and six-coordinate loose-contact pair (LCP) (Figures 2 and 8 of the main text, respectively). For completeness, representative snapshots of all the different coordination numbers, extracted from the Umbrella Sampling simulations, are plotted in Figure 1. For clarity, we plot only the first solvation shell THF molecules, which are defined as those molecules within a distance of the electron center-of-mass (COM) that corresponds to the first minimum in the THF COM–electron COM radial distribution function. These first-solvation-shell radii, which are different for each Na^+ coordination number, are presented in Table III.

TABLE III. First solvation shell radii of the neutral sodium species in THF (from the minimum in the THF COM–electron COM radial distribution function) for each Na^+ coordination species

n_{Na^+}	0	1	2	3	4	5	6
$r_{\text{min}} \text{ (\AA)}$	7.0	6.7	6.0	5.7	5.6	6.1	6.8

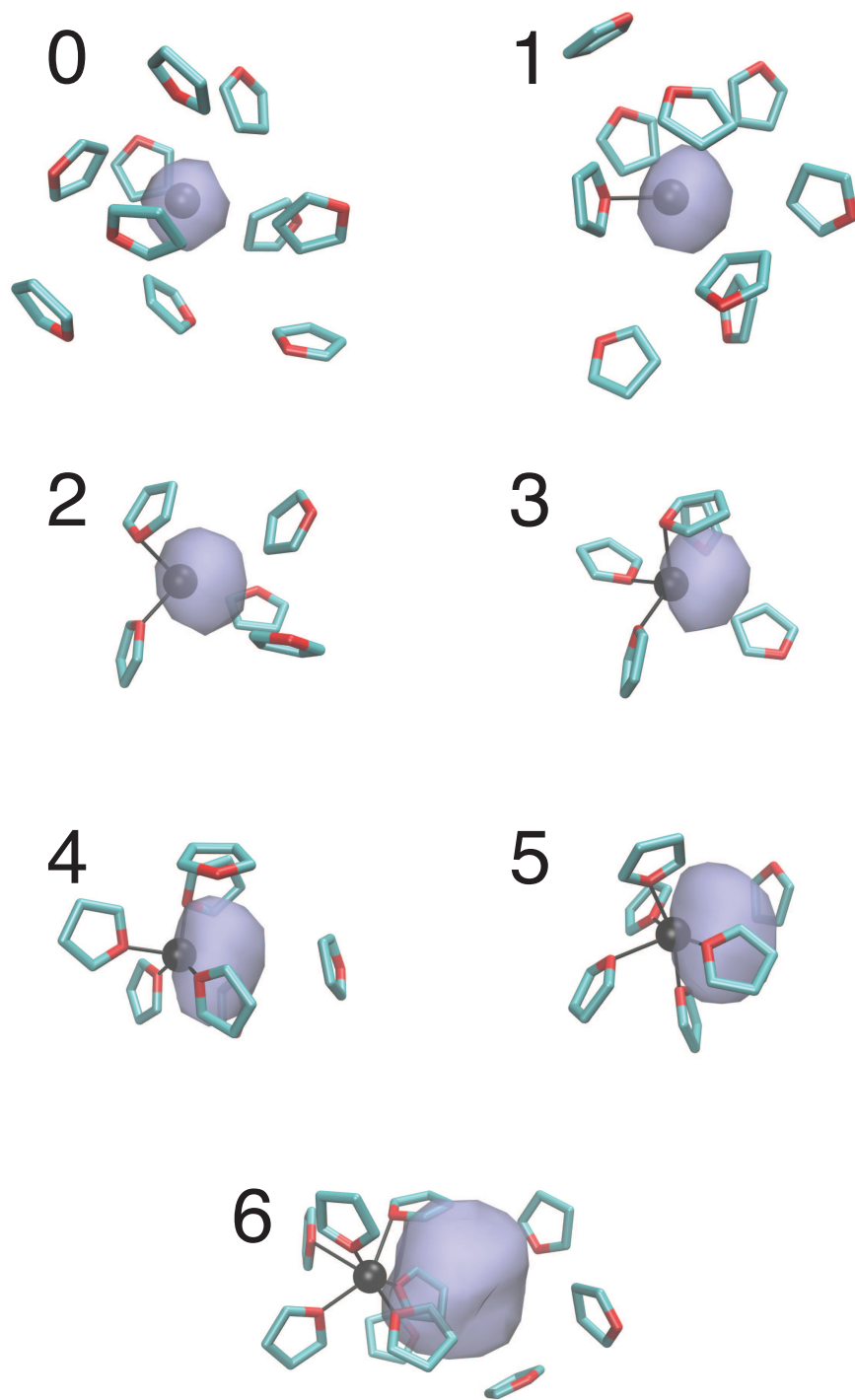


FIG. 1. Molecular dynamics snapshot of the equilibrium neutral sodium species in THF with varying Na^+ coordination numbers (indicated by the number above each plot). The first solvation shell THF molecules are plotted as licorice, the Na^+ core as a black sphere (scaled to its ionic radius) and the valence electron is represented as a translucent blue surface enclosing 50 % of the charge density. Bonds are drawn between Na^+ and THF oxygen sites within 3.65 Å.

EQUILIBRIUM FLUCTUATIONS IN THE TCP COORDINATION NUMBER

At equilibrium, the sodium TCP is predominantly four-fold coordinated, however, both the three-fold- and five-fold-coordinated species are higher in free energy by only $\sim 2.5 k_B T$ (see Figure 4 of the main text) and therefore have appreciable population at equilibrium. Indeed, from our 1-ns simulation trajectory, we observed fluctuations between coordination numbers three, four and five. A time trace of this behavior is shown for the entire trajectory in Figure 2(a) and for an expanded 100-ps temporal region in Figure 2(b). From this figure, we estimate the lifetimes of three-fold- and five-fold coordinated species to be on the order of a few picoseconds, in general agreement with the time scales extracted from recent pump-probe transient hole-burning spectroscopy measurements.[9]

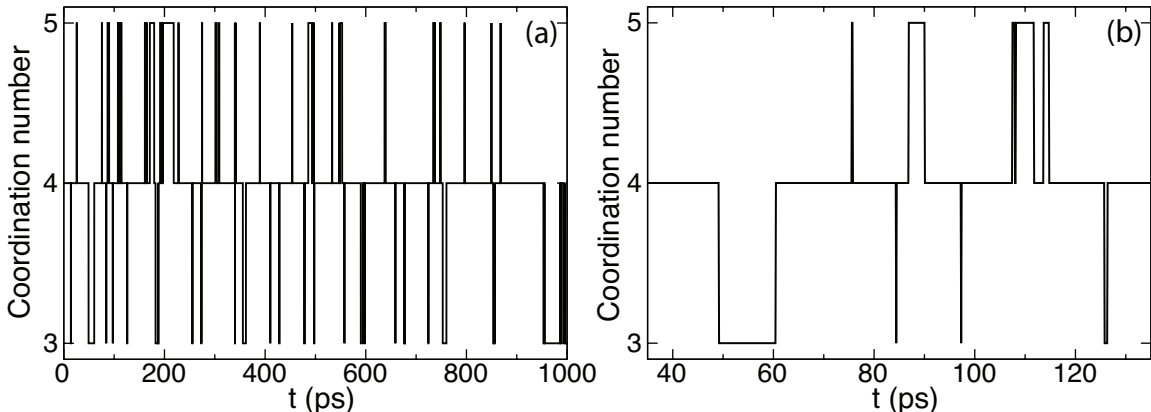


FIG. 2. Instantaneous coordination number of the sodium TCP from a 1-ns equilibrium simulation. The coordination number is defined as the number of THF oxygen sites within 3.65 \AA of the sodium cation. Panel (a) shows the time trace of the coordination number fluctuations for the entire 1-ns trajectory. Panel (b) expands a 100-ps segment of this trajectory. Clearly coordination numbers three, four and five are in dynamic equilibrium, with average lifetimes of coordination numbers three and five on the order of a few picoseconds.

EFFECT OF TEMPERATURE AND DENSITY ON THE PROPERTIES OF THE TCP

The simulations of the sodium TCP presented in the main text were performed at room temperature and density in the canonical ensemble. It is known experimentally that the absorption spectra of alkali metal tight-contact-pair species shift to resemble those of loose-contact-pair species (i.e. higher coordinated alkali cations) upon lowering the temperature. In Section 3.2 of the main text, we suggested this behavior could be understood in light of the balance between entropy favoring low coordination numbers of the alkali cation and the potential energy favoring higher coordination numbers. However, this analysis assumes that the coordination energy and entropy terms are temperature independent, which is unlikely to hold over the broad range of temperatures accessed experimentally (from ~ 170 to 298 K). Thus to gain insight into the behavior of the sodium TCP with temperature, we ran a preliminary 500-ps long simulation at 173 K at the experimental density of THF at this temperature of 1.002 g cm^{-3} . To isolate the effects of temperature and density, we also ran a 500-ps long simulation at this higher density but at room temperature.

Figure 3(a) shows a time trace of the coordination number of the Na^+ from the higher density, 173 K simulation. Here we see that the TCP is almost exclusively five-fold coordinated, in contrast to the predominantly four-fold coordinated TCP at room temperature. Thus, our interpretation of the temperature dependence of the alkali TCP’s spectrum as being a result of changes in coordination number is borne out by simulation. However, the increase in coordination number can not be considered an effect of temperature alone. Figure 3(b) shows a time trace of the coordination number of Na^+ at 298 K with the increased density of 1.002 g cm^{-3} . At this temperature and density, the TCP is predominantly four-fold coordinated; however, coordination number 5 appears to be more prevalent than what was seen at ambient density (relative populations of the three-, four-, and five-fold species are 1:77:22 at $\rho=1.002 \text{ g cm}^{-3}$ versus 9:84:7 at $\rho=0.8892 \text{ g cm}^{-3}$; see also Figure 2, above). This stabilization of higher coordination numbers at higher density is likely due to the fact that the electrostrictive interactions of the THF solvent molecules with the sodium cation increase when the solvent is at a higher density. Thus, the shift to higher coordination numbers with lower temperature is a result of both the lower temperature reducing the entropic penalty to forming high coordination numbers and the increased density, which

because of electrostriction, stabilizes greater charge separation of the contact pair. Finally, we note that although these findings agree with experimental trends, the OPLS model of THF was parameterized only for ambient conditions, so one should use caution when trying to extract any quantitative results from these preliminary simulations. We leave a more detailed analysis of the temperature dependence of the sodium TCP to future work.

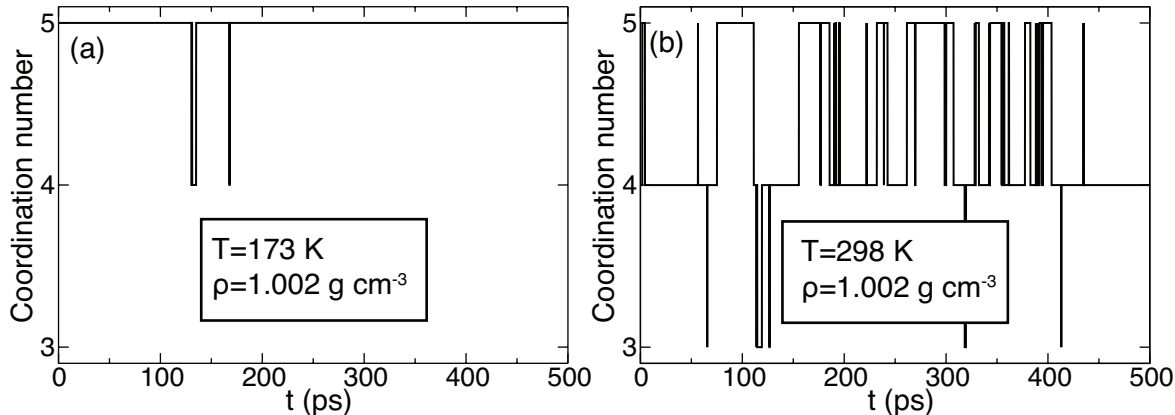


FIG. 3. Effect of temperature and density on the instantaneous coordination number of the neutral sodium species in THF. Panel (a): same as Fig. 2(a) but taken from a 500-ps equilibrium simulation at a temperature of 173 K and a density of 1.002 g cm^{-3} . Panel (b): as in panel (a), but taken from a 500-ps equilibrium simulation at a temperature of 298 K and a density of 1.002 g cm^{-3} . The sodium species remains a TCP under these conditions; however, lowering the temperature and increasing the density both increase the proportion of five-fold coordinated species relative to ambient conditions.

-
- [1] M. J. Bedard-Hearn, R. E. Larsen, and B. J. Schwartz, J. Phys. Chem. B, **107**, 14464 (2003).
 - [2] M. J. Bedard-Hearn, R. E. Larsen, and B. J. Schwartz, J. Chem. Phys., **122**, 134506 (2005).
 - [3] M. J. Bedard-Hearn, R. E. Larsen, and B. J. Schwartz, J. Chem. Phys., **125**, 194509 (2006).
 - [4] W. J. Glover, R. E. Larsen, and B. J. Schwartz, J. Chem. Phys., **132**, 144102 (2010).
 - [5] G. Ciccotti, M. Ferrario, and J.-P. Ryckaert, Mol. Phys., **47**, 1253 (1982).
 - [6] M. P. Allen and D. J. Tildesley, *Computer Simulation of Liquids* (Oxford University Press, London, UK, 1992).
 - [7] K. A. Feenstra, B. Hess, and H. J. C. Berendsen, J. Comput. Chem, **20**, 786 (1999).
 - [8] H. C. Andersen, J. Comp. Phys., **52**, 24 (1983).
 - [9] A. E. Bragg, W. J. Glover, and B. J. Schwartz, Phys. Rev. Lett., **104**, 230005 (2010).